EXPERIMENTS ON THE FORCED WAKE OF AN AIRFOIL
TRANSITION FROM ORDER TO CHAOS

88-3840-CP

K. Stuber* & M. Gharib+
University of California, San Diego
La Jolla, CA 92093

ABSTRACT

Presented here is an experimental effort which attempts to understand the nature of the wake of an airfoil in a controlled environment. The frequency of oscillation in the wake (the vortex shedding frequency) is controlled through the introduction of an external perturbation. Strip heaters are used to introduce waves into the top and bottom boundary layers of a thin symmetric airfoil which are amplified and introduced to the wake. The linear and nonlinear interactions of these waves in the wake are studied in detail. Three modes of interaction have been observed through flow visualization and velocity measurements: frequency locking in which the vortex shedding frequency is the same as the forcing frequency, quasiperiodic vortex interaction in which periodic clusters of vortices are observed in the wake, and chaotic vortex interaction in which the vortices in the wake have a three dimensional random structure.

Two points of view are applied in the analysis of the data:

1. The effect of forcing on flow parameters such as velocity fluctuations and drag are examined.

2. Ideas from nonlinear dynamics (such as Lyapunov exponents and Poincaré sections) are applied in an attempt to relate the basic physics of the system to the concepts of mode interaction and chaos.

INTRODUCTION

The understanding of the basic dynamics of wakes is of primary interest in the field of fluid dynamics, from both a basic research and an engineering point of view. For many engineering purposes, it is advantageous to improve the characteristics of the system (for example, to reduce the drag or delay the transition to turbulence). However, it is difficult to understand complex systems such as wakes without making simplifications. Through the introduction of external control, one can obtain a better environment for examining the nature of the system by establishing a greater number of known parameters. The advantages of forcing are twofold. The introduction of a known perturbation to the flow provides a reference for the nature and intensity of the predominant disturbance which precipitates the natural transition. In addition, the reproducibility of the transition process is greatly enhanced.

Presented here is an experimental effort which attempts to understand the nature of the wake of a thin airfoil in a controlled environment. The frequency of oscillation in the wake (the vortex shedding frequency) is controlled through the introduction of an external perturbation. Due to the fact that the wake is a dynamic system, an active control technique which does not change the overall characteristics of the flow was implemented. The strip heater technique which was first introduced by Liepmann *et al*[1,2] for flat plate boundary layers and by Gharib[3] for shear layers is used to excite Tollmien-Schlicting waves in the airfoil boundary layers (fig. 1). The waves are amplified by the boundary layer and then introduced to the wake. The linear and nonlinear interactions of these waves in the wake are the primary interest of this study. To our knowledge this is the first set of experiments in which the strip heater technique is used in a flow which contains both signs of vorticity (i.e. a wake).

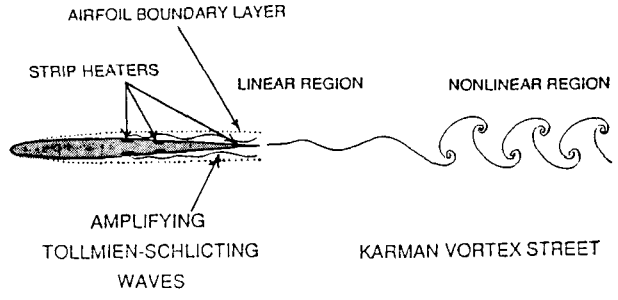

Figure 1 - The strip heater technique for introducing waves into the wake of an airfoil

The introduction of external perturbations to a flow requires a complete understanding of the receptivity of the system to the forcing frequencies. The response of the wake to a range of input frequencies needs to be established. A study of the response of the wake to the introduction of external frequencies is presented in the initial sections of this paper. Once the wake response to a single frequency is established, a more detailed investigation of the flow characteristics of a multiple frequency system can be performed.

The analysis of a multiple frequency system leads naturally to a discussion of the nonlinear dynamics of the system. In recent years, attempts have been made to explain the transition from laminar to turbulent flow in terms of ideas from the relatively new field of nonlinear dynamics. Some nonlinear systems which are described as "chaotic" have the interesting property that they produce essentially unpredictable behavior even though the governing equations of motion are deterministic. Many examples of chaotic behavior have been observed in fluid mechanical systems whose governing equations (the Navier-Stokes equations) are nonlinear due to the presence of the advection terms. The most extensive documentation of chaotic behavior in hydrodynamic systems exists for two experiments*: Rayleigh-Benard convection and Taylor-Couette flow which are examples of fully bounded (closed) flows. It has been observed that for some conditions the transition to chaotic states and to turbulence in these fully bounded fluid flows occurs according to scenarios generally associated with low order dynamical systems. The question arises as to whether there is a correspondence between the behavior of these low order dynamical systems and the transition to turbulence in open fluid systems such as wakes, shear layers, and boundary layers even though in theory, these closed fluid mechanical systems have an infinite number of degrees of freedom.

* Post-Graduate Researcher, Member APS
+ Assistant Professor, Dept. of AMES
Member AIAA, APS, ASME

*For an extensive list of references on these flows, see Gollub & Benson[4] and Swinney[5]

The search for chaotic behavior in open systems has focused on the wake of a thin cylinder. Sreenivasan[6] reported the existence of "windows of chaos" in the laminar wake of a cylinder at certain values of the Reynolds number. Much discussion has been focused on the nature of the chaotic interactions observed. Van Atta & Gharib[7] demonstrated convincingly that the chaotic state observed by Sreenivasan was the result of an aeroelastic coupling between the cylinder vibration modes and the vortex wake. An additional control parameter was contributing to the system - the tension on the cylinder which dictates the vibration modes. The results of Van Atta & Gharib were supported by the recent numerical work of Karniadakis & Triantafyllou[8] which showed that the natural cylinder wake in the absence of external forcing does not exhibit chaotic behavior in the laminar range. The only frequency observed was that which was selected by the absolute instability mechanism of the mean flow. Aperiodic states were observed only in the presence of periodic forcing.

Due to the coupled nature of the wire/wake system, the amplitude and frequency of forcing could not be independently controlled by the investigators. Presented here is a series of fully controllable experiments in which the interaction of multiple independent frequencies in an open flow (the wake of an airfoil) is examined. Various behaviors associated with the Ruelle-Takens-Newhouse ("RTN")[9] or three frequency route to chaos are observed. Standard diagnostics from nonlinear dynamics (Poincaré sections and Lyapunov exponents) are applied to the experimental data to establish the dynamical nature of the system. In addition, the flows are also examined from a classical fluid dynamics point of view (flow visualization, velocity and drag measurements, wavenumber spectra) to show that a connection can be established between laminar chaotic flows and the onset of turbulent flow.

EXPERIMENTAL DETAILS

The experiments were performed in the UCSD department of Applied Mechanics & Engineering Sciences water tunnel. The water tunnel has an 8 foot long test section with a 10" square cross section.

A thin symmetric airfoil (NACA 63A008) was mounted 12.7 cm (5") from the entrance to the test section. The airfoil chord measured 7.6 cm (3"), the thickness was 0.64 cm (0.25"), and the span was 24.1 cm (9.50"). Thin stainless steel strips (0.002" thick, 0.10" wide) were flush mounted on the top and bottom surfaces of the airfoil at the 1/2, 2/3, and 23/24 chord point of the airfoil. Each strip was connected to an independent power supply which was driven by a signal generator. Dye ports were located at the center of the airfoil on the top and bottom of the leading edge. To visualize the flow, dye was gravity fed to the injection tubes and discharged into the airfoil boundary layers.

OPERATIONAL PROCEDURES / DEFINITIONS

Flow velocities were measured with a single component laser Doppler anemometer. A dual beam forward scatter configuration was used to measure the downstream component of velocity (u). The velocity time series was digitized and stored on a MASSCOMP data acquisition system for further processing. Power spectra were computed from the digitized time series according to conventional signal processing techniques. Real time power spectra of the velocity signal were obtained on a Hewlett Packard dynamic signal analyzer.

Measurements were made at a flow speed of 11.5 cm/s. The Reynolds number based on the model chord length is 8600. The origin of the reference system is located at the trailing edge of the airfoil which was positioned with zero angle of attack. The x-axis is in the flow direction and the y-axis is in the cross-stream direction. The velocity and length scales incorporated in the analysis of the experiment are U_∞, the freestream velocity, and δ , the wake width measured from the wake centerline (y=0) to the point where $u = .99U_\infty$. For natural flow (unforced) at x/c = 1, δ = 0.515 cm resulting in a Reynolds number based on δ (Re_δ) of 590.

STRIP HEATER TECHNIQUE

Perturbations are introduced to the boundary layer of the airfoil through the use of strip heaters. Metal strips are flush mounted on each side of the airfoil. A sinusoidal electric current is applied to the strip heater which results in a local change of the viscosity of the fluid in contact with the strip. It can be shown[10] that the modulation of the viscosity by temperature has the same effect as blowing or suction of the fluid. For periodic heating, the effective sinusoidal displacement of the streamlines is convected downstream by the mean flow velocity.

From linear boundary layer stability theory, it is known that only a finite range of perturbation frequencies will be amplified by the boundary layer. It is this range of frequencies that is forced using the strip heater technique. Due to the quadratic joule heating effect, it is necessary to generate an input signal at one-half the desired output frequency. In addition each frequency must be input on a separate strip.

RESULTS AND DISCUSSION

RECEPTIVITY

The first step in examining a forced wake is to introduce a single frequency into the flow and to monitor the wake response. By sweeping over a range of frequencies near the natural vortex shedding frequency, a receptivity curve is constructed by measuring the response power in a narrow band (bandwidth = 0.1 Hz) centered at the forcing frequency. This power is a measure of the bandwidth $\overline{u'^2}$ for the frequency. The sum of the power in all frequencies is equal to the square of the rms velocity. The input power to the strip is held constant when constructing the curve. The receptivity curve (measured at y = δ of the natural wake) is normalized by the maximum value obtained for the set of measurements. Due to the fact that the trailing edge strip has no boundary layer for the amplification of the perturbations,

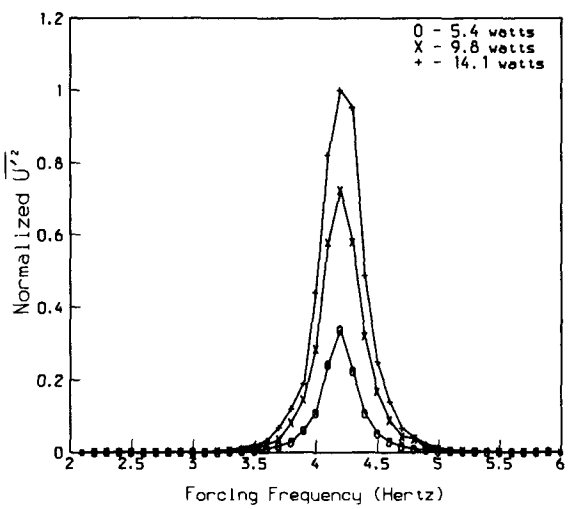

Figure 2 - Receptivity for three input power levels (at x/c = 3 and y = δ)

the experiments were performed using the strips located near the center-chord point of the airfoil. The role of the forcing power level using the top middle strip is examined in figure 2. As the power increases, the range of amplified frequencies expands and a greater maximum amplification value is attained. The most amplified frequency is 4.25 Hz which is very close to the natural vortex shedding frequency. For a range of frequencies near the natural frequency, the vortex shedding frequency tracks or "locks" onto the forcing frequency. Frequencies for which this occurred were considered to be in the "locking range." A formal definition of locking range was established : locking resulted when the amplitude of the bandwidth $\overline{u'^2}$ for the forcing frequency exceeded that of the natural by one order of magnitude. As the power of forcing increases, a greater number of frequencies are included in the locking range (fig. 3).

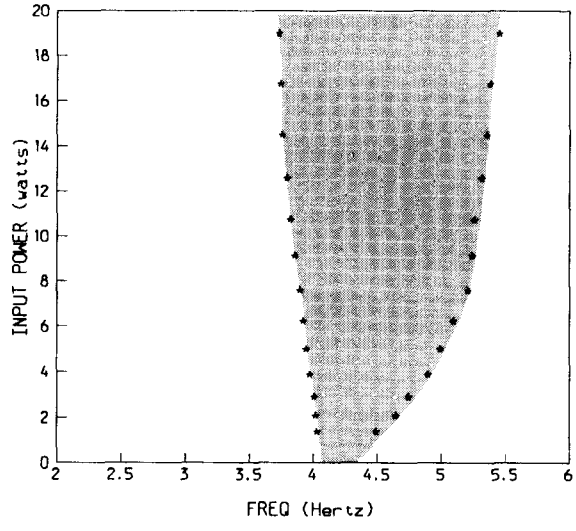

Figure 3 - The locking range (at x/c = 3 and y = δ)

THREE FREQUENCY ROUTE TO CHAOS

In the case of single frequency forcing, the main parameters varied were the amplitude and frequency of forcing. By fixing one of the parameters (e.g.,the amplitude), the effect of the second parameter was determined by sweeping it over a range of values. This type of procedure led to the results of the receptivity and locking ranges. With the addition of a more frequencies, the behavior of the system became increasingly complex as the frequencies interacted. In order to determine the nature of the interactions, a flow mapping was performed which examined combinations of multiple frequencies. Before examining any forced cases, it should be noted that the natural frequency in the unforced flow is relatively broadband. (fig. 4) In order to avoid any complications associated with the broadband nature of the natural frequency, the natural frequency was forced at a relatively low level resulting in a clean peak.

Presentation of selected cases. In the following section, a representative sequence from order to chaos is presented and submitted to a range of diagnostics to determine the dynamical nature of the system. The power spectrum and time series for each case (at $y = \delta$) are presented in figures 5 through 8.

The best example of an ordered flow is one in which the most amplified frequency (4.2 Hz) is forced at a relatively high amplitude (10 W). The power spectrum (fig. 5) exhibits sharp peaks at the primary frequency and its second harmonic. The time series is very uniform for the locked case. The next step in the transition is a strongly quasiperiodic case where the two frequencies in the locking range ($f_1 = 4.2$ Hz, $f_2 = 4.4$ Hz) are

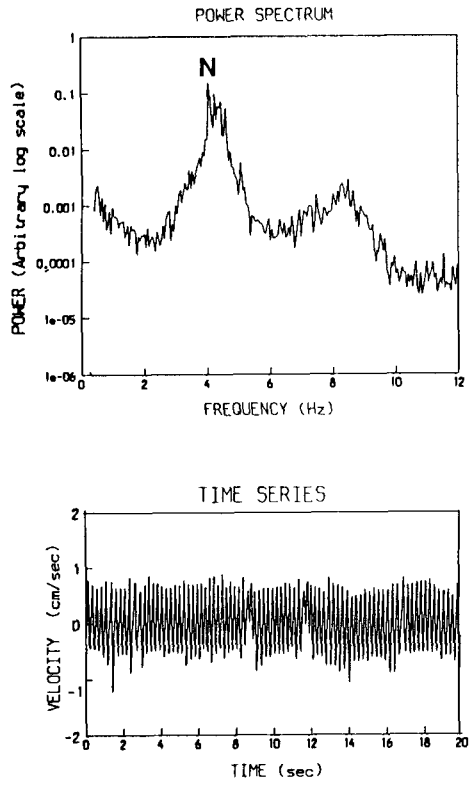

Figure 4 - Power spectrum and time series for the natural case (at x/c = 3 and y = δ)
(Arbitrary scale is consistant for all power spectra)

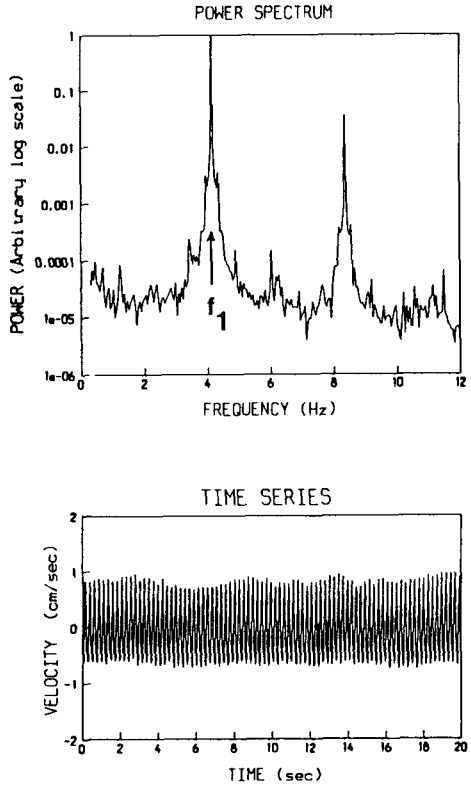

Figure 5 - Power spectrum and time series for the locked case (at x/c = 3 and y = δ)

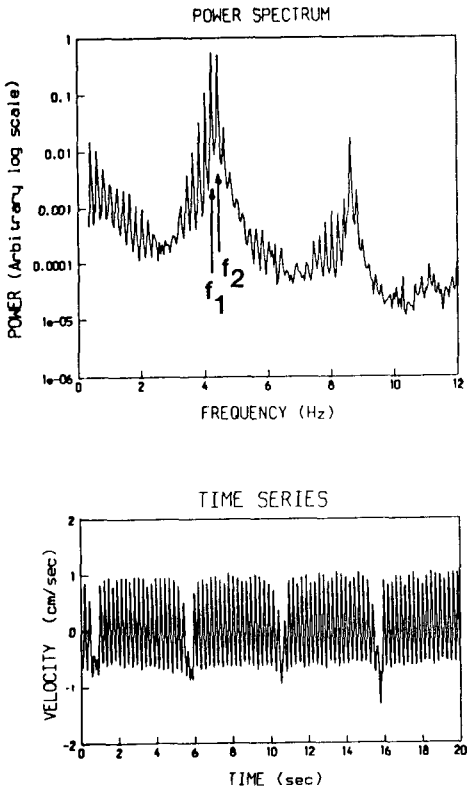

Figure 6 - Power spectrum and time series for the strongly quasiperiodic case (at x/c = 3 and y = δ)

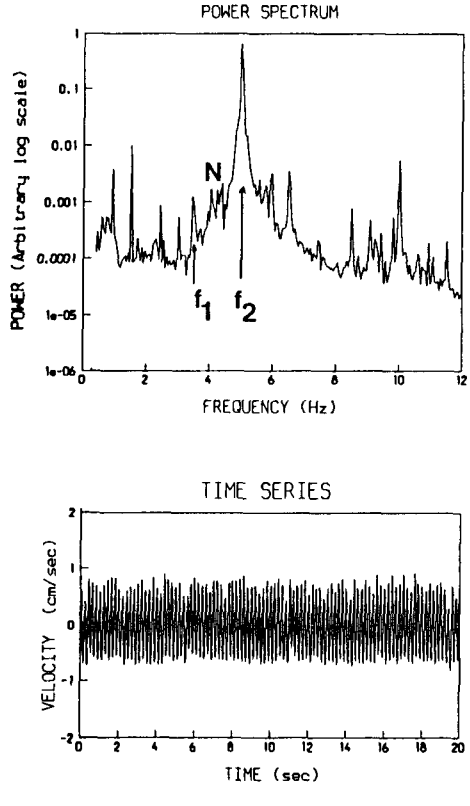

Figure 7 - Power spectrum and time series for the weakly quasiperiodic case (at x/c = 3 and y = δ)

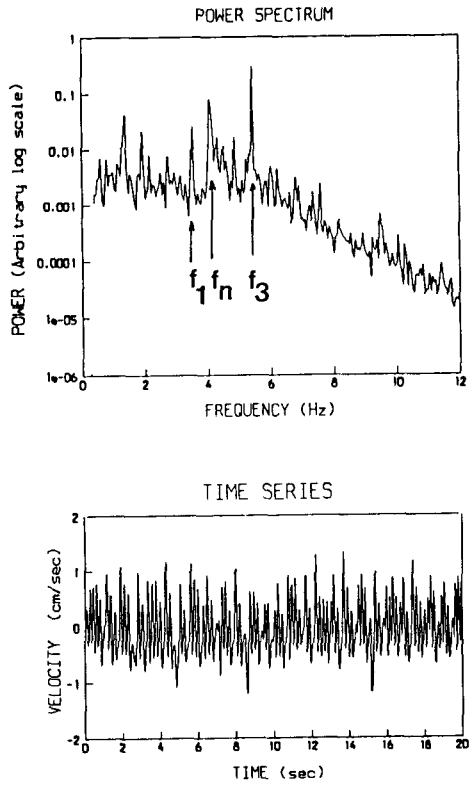

Figure 8 - Power spectrum and time series for the chaotic case (at x/c = 3 and y = δ)

forced such that their response amplitudes in the power spectrum are equal. The resulting power spectrum (fig. 6) contains interaction peaks at many linear combinations of the two forcing frequencies. The velocity time series exhibits a strong beating pattern associated with the difference between the two forcing frequencies. From strongly quasiperiodic, one moves next to a weakly quasiperiodic case which shows some signs of irregular behavior. The two forcing frequencies are selected near the edge of the locking range (f_1 = 3.5 Hz, f_2 = 4.9 Hz). The higher frequency is allowed to dominate the flow, while the lower frequency is just strong enough to result in some interactions. The power spectrum (fig. 7) shows a couple of interaction peaks. The natural frequency is present which explains the appearance of a peak near 1.0 Hz. In the time series, a beat frequency of 1.7 Hertz corresponding to the difference between the forcing frequencies is evident. The final stage of the transition from order to chaos is obtained by forcing the natural frequency in addition to two frequencies slightly outside of the locking range (f_1 = 3.5 Hz, f_2 = 5.42 Hz, $f_3 = f_n$ = 4.075 Hz). The input amplitudes of the frequencies were set such that the responses of the three frequencies in the power spectrum were roughly the same order of magnitude. The three frequencies are incommensurate. For this final case, a distinct change in the nature of the power spectrum (fig. 8) occurs. In additions to peaks at the three forcing frequencies and their linear combinations, there is a significant increase in the background noise level by two orders of magnitude relative to the locked case. The noise level for this last case is even higher than the noise in figure 7 in which the natural frequency is also present. The time series are very irregular with no distinct periodicity. Using the power spectrum as a primary diagnostic, it would appear that the three frequency case

behaves chaotically. However, due to the lack of phase information from the power spectrum, further diagnostics from the field of nonlinear dynamics must be applied to the data before a definitive classification is made.

THE NONLINEAR DYNAMICAL ANALYSIS

Phase Space Reconstruction. The first step in analyzing experimental data obtained from a dynamical system is to construct the phase space of the system. Given a time series of a single quantity, U(t), (in the current experiment, the x-component of velocity), a reconstruction of the phase space can be obtained by using a time delay technique[11,12] so that

$$\vec{X}(t) = \{U(t), U(t+\tau), \ldots, U(t+(m-1)\tau)\}$$

where τ is the time delay and m is the embedding dimension (or anticipated number of variables needed to characterize the motion of the system) For the current experiment, an embedding dimension of 5 was selected (which, it was felt, would be more than sufficient for the locked and quasiperiodic cases, but not necessarily enough for the chaotic case.) Although any time delay may be selected, it is preferable to select one corresponding to 1/2 - 1 1/2 orbital periods. For the present work, a time delay of 42 points (0.17 sec = 0.67 orbital period) was utilized.

The phase space reconstructions (phase portraits) for the natural (unforced) wake and the locked and chaotic wakes are presented in figures 9 to 11. Due to constraints of the graphics system, only the first 5000 points are plotted. However, the nature of the trajectories for each condition did not change when the plots with 22500 points were viewed on a higher level graphics system. In each figure, the phase portrait is generated from a time trace at $y = \delta$. The coordinates for the axes are the binary values obtained from the data acquisition system. The value 900 corresponds roughly to 9 cm/sec, 1300 to 13 cm/sec, and so on. In the transition from natural to locked flow (figs. 9 to 10), the organizing of the phase portrait is evident. Random noise is suppressed in the locked case as was seen previously in the power spectrum. The locked portrait resembles a thin cord or torus. A distinct change in the phase portrait occurs as the flow becomes chaotic. The chaotic phase portrait (fig. 11) resembles tangled balls of yarn rather than thin ribbons.

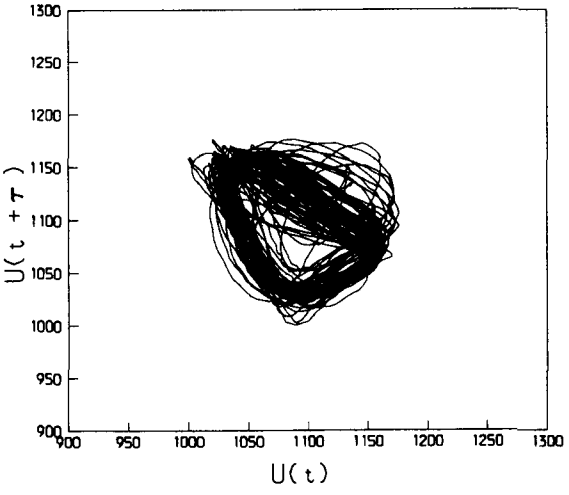

Figure 9 - Phase space reconstruction for the natural case (at x/c = 3 and y = δ)

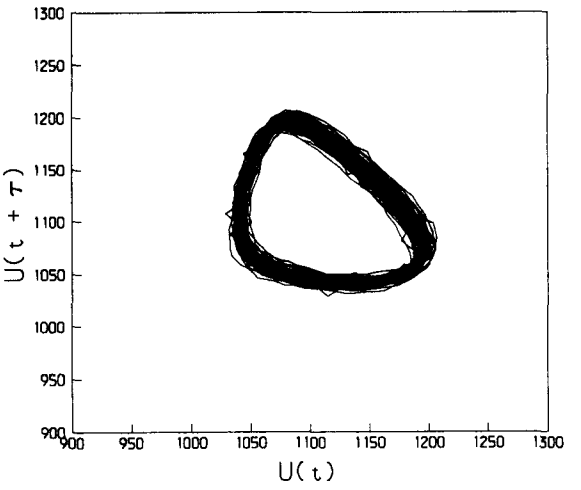

Figure 10 - Phase space reconstruction for the locked case (at x/c = 3 and y = δ)

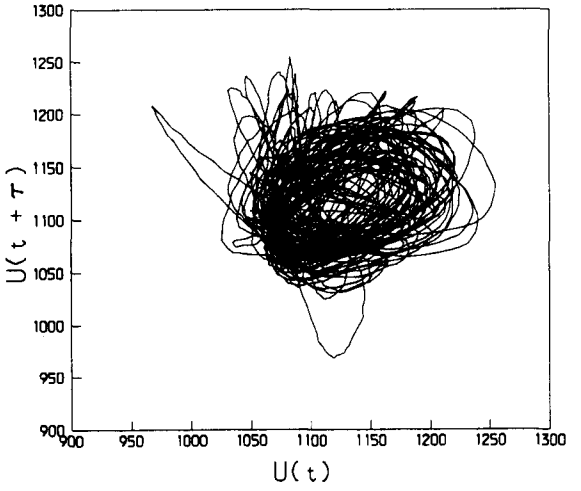

Figure 11 - Phase space reconstruction for the chaotic case (at x/c = 3 and y = δ)

Poincaré Sections. Once the phase space reconstruction is complete, the intersection of trajectories (in the first three dimensions) with a plane can be examined. The set of points intersecting the plane constitutes a Poincaré section of the system. The Poincaré section of the locked case was characterized by concentrations of points at the intersection of the torus with the plane. The intersections of the chaotic case were randomly scattered across the plane.

Lyapunov Exponents. The phase space reconstruction and Poincaré sections provide information about the geometrical nature of the system. To complement those results, quantitative details can be obtained from the reconstructed phase space by measuring the spectrum of Lyapunov exponents of the system (originally defined by Oseledec[13]). Lyapunov exponents quantify the sensitivity of a dynamical system to initial conditions. By considering the largest exponent λ_1, the dynamical nature of the attractor can be determined. If $\lambda_1 < 0$, all initial conditions eventually converge to the same point, a fixed point. $\lambda_1 = 0$

implies the length of the principle axis remains constant. This corresponds to a limit cycle (either periodic or quasiperiodic motion). If $\lambda_1 > 0$, lengths are diverging (typically at an exponential rate). When such a condition exists, the attractor is said to be "strange" or "chaotic." The values of the largest Lyapunov exponent for the experimental time series is determined according to an algorithm developed by Wolf, Swift, Swinney, and Vastano[14].

To quantify the nature of the flows as a function of position across the wake, the largest Lyapunov exponent was measured at several points across the wake to form a "Lyapunov profile". In presenting the profiles, a three point average was performed to smooth out fluctuations. A comparison of the four order-to-chaos cases (fig. 12) demonstrates that the dynamical behavior of the chaotic case is indeed different than the three ordered cases. The chaotic exponents are typically three times greater than the exponents for the ordered cases. On average, the locked exponents are lower than the two quasiperiodic cases. The increase of the exponents at the edges of the profiles may be attributed to the effect of freestream noise.

Summary of nonlinear dynamics diagnostics. Through the use of phase portraits, Poincaré sections, and Lyapunov exponents, a distinct transition is seen from ordered to chaotic flow. The non-zero values of the Lyapunov exponents for the ordered cases are attributed to noise inherent in an open system.

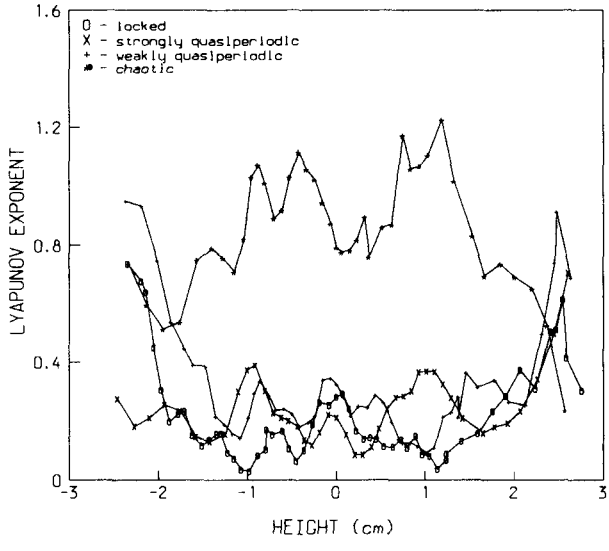

Figure 12 - Lyapunov exponent as a function of height for the route to chaos cases (at x/c = 3)

THE FLUID DYNAMICS OF A CHAOTIC WAKE

The numerical diagnostics provide a measure of a system's divergence. Left unanswered is the question of the effects of chaos on flow parameters such as the vortex configuration, the mean and fluctuating velocities, and the drag.

Flow visualization. Flow visualization reveals the vortex configuration of the wake. A locked flow (fig. 13) is characterized by the uniform staggered vortex pattern known as the Kármán vortex street. The second photo in the sequence (fig. 14) presents a quasiperiodic flow which is identified by the existence of uniform vortex clusters. The flow visualization corresponds to the second quasiperiodic case. The short wavelength of the almost identical clusters is due to the difference frequency of 1.4 Hz. Within the clusters, pairing of the vortices is occurring. To complete the sequence, the chaotic case is presented in figure 15. A random nature to the vortex patterns exists. At times segments of the Kármán street are visible; at other times, a great deal of stretching and diffusion is present. In light of the fact that patches of order exist, it can be said that the chaos is a result of the clash of orders rather than the lack of order.

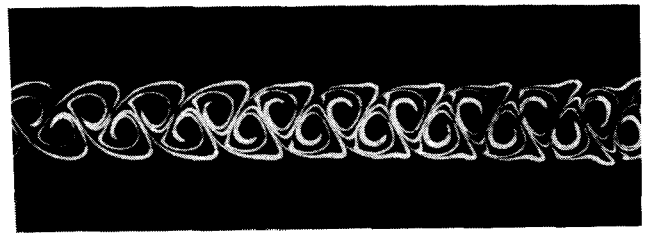

Figure 13 - Flow visualization of locked case

$(f_1 = f_n = 4.075\ Hz)$

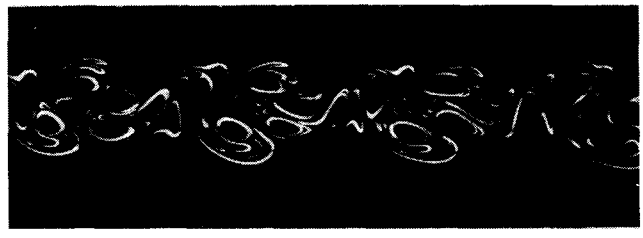

Figure 14 - Flow visualization of quasiperiodic case

$(f_1 = 3.5\ Hz\ , f_2 = 4.9\ Hz)$

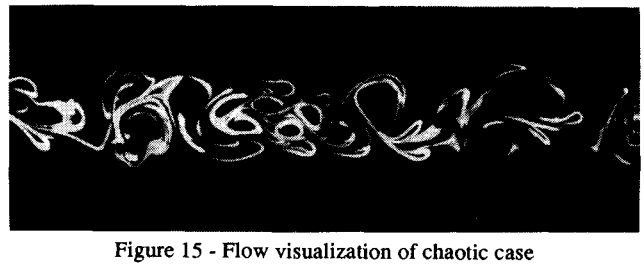

Figure 15 - Flow visualization of chaotic case

$(f_1 = 3.5\ Hz\ , f_2 = 5.42\ Hz\ , f_3 = f_n = 4.075\ Hz)$

Velocity Parameters and Drag Results. Consider next the velocity measurements. The mean and fluctuating velocity profiles of the locked and chaotic flows are presented in figure 16. The locked case is indicated by the solid line; the chaotic case by the symbols. In examining the mean velocity profile, the chaotic case has a smaller deficit compared to the locked case. A more dramatic difference between the locked and chaotic cases appears in the rms ($\sqrt{u'^2}$) profiles. The locked $\sqrt{u'^2}$ profile is characterized by two maxima corresponding to the positions of the vortex cores in the Kármán vortex street. The chaotic profile contains a third peak (an overshoot) on the centerline of the wake. The increased fluctuations at the centerline and the smaller wake deficit for the chaotic case would seem to imply a reduction in drag. However, the profiles presented are measured at x/c = 3 where contributions from the y-component of velocity become significant. To determine the drag coefficient of the locked and chaotic cases, a control volume analysis was applied to velocity profiles measured at x/c = 1 (where the assumption of $\overline{V} = 0$ is valid). The drag coefficient for the locked case revealed a reduction of drag by 15% relative to the natural case. Similar reductions in drag have been seen[15] but only in the presence of high amplitude forcing. The chaotic case resulted in a 4% increase in drag when compared to the natural case. This is a relatively insignificant change.

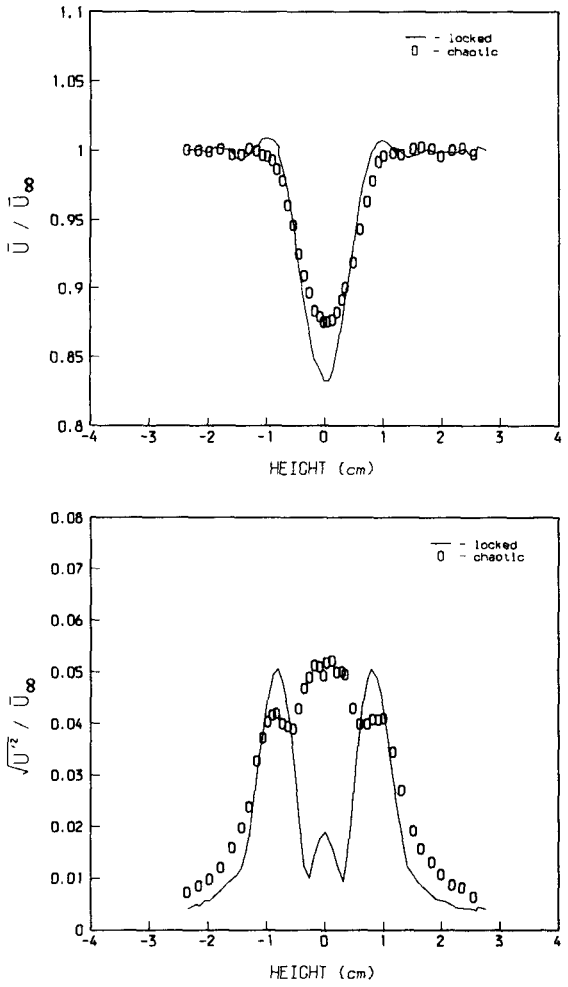

Figure 16 - Mean (top) and rms (bottom) velocity profiles for the locked and chaotic cases (at x/c = 3)

CHAOS & TURBULENCE - ARE THEY RELATED?

When examining the flow visualization for the chaotic case, a range of scales of motion is apparent, and some areas with strong mixing exist. For the chaotic case, it was observed that three dimensional motion (out of the picture plane) existed which was not present in the locked case. The chaotic case appeared to contain regions which were locally turbulent. An attempt is made here to determine statistically whether the laminar chaotic case is similar to a fully developed turbulent flow. Using the wavenumber spectrum as a diagnostic, a comparison of the chaotic spectrum to Kolmogorov's"k to the -5/3"[16] law is performed. For isotropic turbulence, the wavenumber magnitude spectral density $E(k)$ can be related to the wavenumber k by $E(k) \propto k^{-5/3}$. The quantity measured in the experiment is the Fourier power spectrum $\phi(\omega)$ where ω is radian frequency. Bradshaw[17] indicates that for most purposes $\phi(\omega)$ can be used as an approximation to $\phi(k_1)$ which in turn is proportional to $E(k)$. "k_1" is the wavenumber in the downstream direction of the flow. The one dimensional energy spectra, $E(k_1)$, are presented in non-dimensional form (scaled by $(\epsilon\nu^5)^{1/4}$) as a function of non-dimensional wavenumber (k_1/k_d) where k_d is the wavenumber associated with the Kolmogorov length scale (η). The dissipation ϵ was determined from the low Reynolds number approximation $\epsilon \approx \nu u^2/l^2$ where u is the typical fluctuation velocity (the rms velocity) and l is the size of the largest eddy in the flow. Other estimations for ϵ were performed with relatively little change to the results.

The wavenumber spectra for the chaotic case at $y = \delta$ and at the centerline are shown in figures 17 & 18 with a log-log scaling. The results at $y = \delta$ show a -6 slope. In contrast, the centerline line spectrum results exhibit a -5/3 slope. An analytical curve by Pao[18] and some experimental data points for low Reynolds number (based on the Taylor microscale) turbulent flows of Uberoi & Freymuth[19] and Comte-Bellot & Corrsin[20] are plotted on the centerline spectrum. It is seen that there is a considerable agreement between the chaotic case and the turbulent cases. The spectrum results indicate that a local behavior exists which shares the -5/3 decay characteristic of a fully turbulent flow. This is quite surprising when one remembers that the flow is a low Reynolds number (Re_δ) 'laminar' flow and that the flow is anisotropic.

To reinforce the concept that the chaotic flow is not globally turbulent, a turbulent wake was created by tripping the airfoil boundary layers. The mean flow velocity was increased to 13

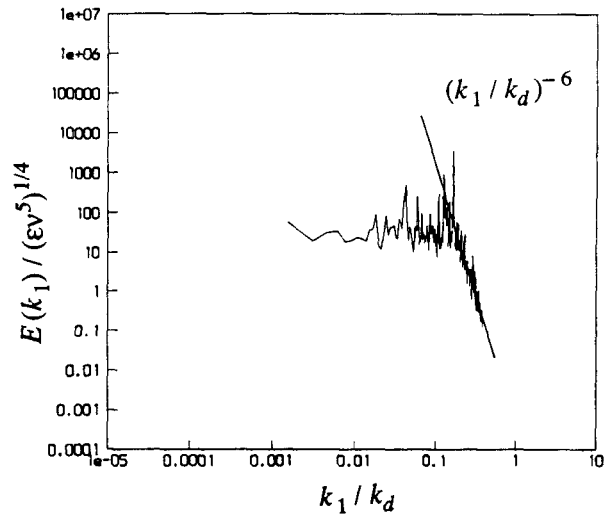

Figure 17 - Energy spectrum of chaotic case at y = δ (at x/c = 3)

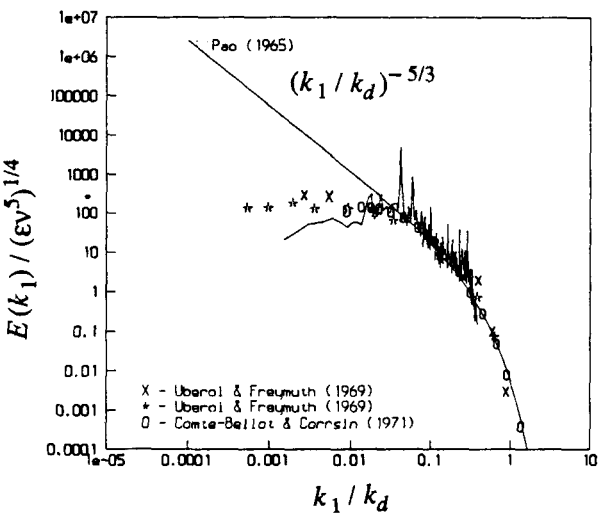

Figure 18 - Energy spectrum of chaotic case at y = 0 (at x/c = 3)

cm/s. The resulting flow (fig. 19) is characterized by the presence of a more uniform range of scales when compared to the chaotic case.

Figure 19 - Flow visualization of a turbulent wake

CONCLUSION

This study has explored the response of the wake to external perturbations. Within the receptivity range, a band of frequencies is identified for which the natural vortex shedding frequency locks onto the forcing frequency. This range is called the "locking" range of the system.

A mapping of the possible behaviors existing in a three frequency flow system is obtained. For the first time, a three frequency route to chaos in an open system is explored. Diagnostics from the field of nonlinear dynamics show a definite transition from order to chaos.

The fluid dynamics of the route to chaos cases is explored. Significant changes to the vortex configuration in the flow are observed. Velocity measurements show an increased $\sqrt{u'^2}$ level along the centerline. No significant change in the drag coefficient relative to the natural wake is seen for the chaotic case although a 15% decrease is seen for the locked case.

In an attempt to make a connection between laminar chaos and turbulence, the wavenumber spectrum for the chaotic case is examined. The spectrum obtained at the centerline of the chaotic wake exhibits a $k^{-5/3}$ scaling. This indicates that the Reynolds number (which for the unforced flow is low) is not the only parameter important in the transition from laminar to turbulent flow. It is interesting to note that only three frequencies were input to the flow to create a system that behaves locally like a system with infinite degrees of freedom. This fact should be of great interest to those modelling turbulent flows.

ACKNOWLEDGEMENTS

This paper is based on the work from the Ph.D. Thesis of K. Stuber which was carried out at the University of California, San Diego. The work was sponsored by the Defense Advanced Research Projects Agency - Applied and Computational Mathematics Program through the University Research Initiative program under contract number DARPA / ONR N00014-86-K-0758.

REFERENCES

1. LIEPMANN, H.W., BROWN, G.L., and NOSENCHUCK, D.M. 1982 Control of laminar instability waves using a new technique. *J. Fluid Mech.*, **118**, p. 187.

2. LIEPMANN, H.W. and NOSENCHUCK, D.M. 1982 Active control of laminar-turbulent transition. *J. Fluid Mech.*, **118**, p. 201.

3. GHARIB, M. 1987 Response of the Cavity Shear Layer Oscillations to External Forcing. *A.I.A.A. Journal*, **25**, p. 43.

4. GOLLUB, J.P. and BENSON, S.V. 1980 Many routes to turbulent convection. *J. Fluid Mech.*, **100**, p. 449.

5. SWINNEY, H.L. 1983 Observations of Order and Chaos in Nonlinear Systems. *Physica 7D*, p. 3.

6. SREENIVASAN, K.R. 1985 Transition and turbulence in fluid flows and low dimensional chaos. in *Frontiers in Fluid Mechanics*, ed. S.H. Davis and J.L. Lumley, p. 41, (Springer, Berlin).

7. VAN ATTA, C.W. and GHARIB, M. 1987 Ordered and chaotic vortex streets behind circular cylinders at low Reynolds numbers. *J. Fluid Mech.*, **174**, p. 113.

8. KARNIADAKIS, G.E. and TRIANTAFYLLOU, G.S. 1987 Frequency selection and asymptotic states in laminar wakes. (submitted to *J. Fluid Mech.*)

9. NEWHOUSE, S., RUELLE, D. and TAKENS, F. 1978 Occurrence of Strange Axiom A Attractors Near Quasi Periodic Flows on $T^m, m \geq 3$. *Commun. Math. Phys.*, **64**, p. 35.

10. NOSENCHUCK, D.M. 1982 Passive and Active Control of Boundary Layer Transition. PhD. thesis. California Institute of Technology.

11. TAKENS, F. 1981 Detecting Strange Attractors in Turbulence. in *Dynamical Systems & Turbulence, Warwick, 1980*, Lecture Notes in Mathematics 898, (Springer, Berlin) p. 366.

12. PACKARD, N.H., CRUTCHFIELD, J.P., FARMER, J.D. and SHAW, R.S. 1980 Geometry from time series. *Phys. Rev. Lett.*, **45**, p. 712.

13. OSELEDEC, V.J. 1968 A multiplicative ergodic theorem. Lyapunov characteristic numbers for dynamical systems. *Trans. Moscow Math. Soc.* , **19**, p. 197.

14. WOLF, A., SWIFT, J.B., SWINNEY, H.L. and VASTANO, J.A. 1985 Determining Lyapunov Exponents from a Time Series. *Physica 16D*, p. 285.

15. KOOCHESFAHANI, M.M. 1987 Vortical patterns in the wake of an oscillating airfoil. AIAA paper # AIAA-87-0111.

16. KOLMOGOROV, A.N. 1941 The local structure of turbulence in incompressible viscous fluid for very large Reynolds numbers. *C. R. Acad. Sci. U.R.S.S.*, **30**, p. 301.

17. BRADSHAW, P. 1971 An Introduction to Turbulence and its Measurements. (Pergamon Press, Oxford).

18. PAO, Y-H, 1965 Structure of Turbulent Velocity and Scalar Fields at Large Wave-numbers. *Phys. Fluids*, **8**, p. 1063.

19. UBEROI, M. S. and FREYMUTH P. 1969 Spectra of Turbulence in Wakes behind Circular Cylinders. *Phys. Fluids*, **12**, p. 1359.

20. COMTE-BELLOT, G. and CORRSIN, S. 1971 Simple Eulerian time correlation of full- and narrow-band velocity signals in grid- generated, 'isotropic' turbulence. *J. Fluid Mech.*, **48**, p. 273.